Journal of Experimental Nanoscience
Publication details, including instructions for authors and subscription information:
http://www.informaworld.com/smpp/title~content=t716100757

Synthesis and study of photoluminescence characteristics of carbon nanotube/ZnS hybrid nanostructures

R. Paul[a]; P. Kumbhakar[a]; A. K. Mitra[a]
[a] Department of Physics, National Institute of Technology, Durgapur-713209, India

Online publication date: 07 July 2010

To cite this Article Paul, R. , Kumbhakar, P. and Mitra, A. K.(2010) 'Synthesis and study of photoluminescence characteristics of carbon nanotube/ZnS hybrid nanostructures', Journal of Experimental Nanoscience, 5: 4, 363 — 373
To link to this Article: DOI: 10.1080/17458080903583923
URL: http://dx.doi.org/10.1080/17458080903583923

Journal of Experimental Nanoscience
Vol. 5, No. 4, August 2010, 363–373

Taylor & Francis
Taylor & Francis Group

Synthesis and study of photoluminescence characteristics of carbon nanotube/ZnS hybrid nanostructures

R. Paul, P. Kumbhakar and A.K. Mitra*

Department of Physics, National Institute of Technology, Durgapur-713209, India

(*Received 2 August 2009; final version received 28 December 2009*)

Single-walled carbon nanotube (SWCNT) samples were rigorously purified by high temperature oxidation, acid treatment, ultrasonication, neutralisation and filtration process. By a very simple wet chemical route, SWCNT bundles were hybridised with freshly prepared ZnS nanocrystals of average size 2.00 nm. Characterisation of the prepared samples was done by scanning electron microscopy, energy-dispersive X-ray spectroscopy, high resolution transmission electron microscopy, Fourier transform infrared ray spectroscopy, Raman spectroscopy and UV-Vis spectroscopy. Photoluminescence (PL) study of the SWCNT/ZnS hybrid structure showed two distinct types of emission patterns depending upon the excitation wavelength, one in the ultraviolet region wavelengths and the other, for the higher excitation wavelength range, when the PL spectrum mostly covered the visible region.

Keywords: SWCNT; photoluminescence; optical properties; ZnS nanocrystals

1. Introduction

The discovery of carbon nanotubes (CNTs) by Iijima [1] offered scope for wide applications in different fields for their unique physical and chemical properties [2]. Surface modification of CNTs with biological, organic and inorganic compounds can significantly influence their physical properties and provide novel properties for practical applications [3]. Optical properties of modified CNTs have attracted much attention of the researchers for quite some time now [4,5]. Studies on luminescent semiconductor nanocrystals (NCs) have been used extensively because of their potential applications in future optoelectronic devices. CNTs modified with semiconductor NCs are more active due to their size dependent optical properties, which enhance potential of their applications in several areas [6–14]. The concept behind the CNT/NC hybrid structure lies in the fact that the combined properties of two functional nanoscale materials yield in a wide range of applications [15–20]. The electronic interaction between CNTs and the external semiconductor layer also plays a crucial role in constructing optoelectronic devices [21,22]. Therefore, varieties of semiconductor nanoparticles, such as CdSe, CdTe, PbSe, CdS, TiO_2, SiO_2 and ZnO have been bound to the surface of CNTs.

*Corresponding author. Email: akmrecdgp@yahoo.com

ISSN 1745–8080 print/ISSN 1745–8099 online

DOI: 10.1080/17458080903583923
http://www.informaworld.com

ZnS is an important wide bandgap II–VI semiconductor, which finds applications in luminescent materials [23,24], infrared windows [25], flat panel displays, photocatalysis [26–28] and photovoltaic devices [29]. ZnS NCs are reported to have unique properties, such as photocatalysis, though photocatalytic activity is very low due to the recombination of electron (e^-)/hole (h^+) pairs generated. Since the excited e^- of the conduction band of the semiconductor photocatalyst could migrate to CNTs, the recombination of the e^-/h^+ pairs could be restrained and thus the photocatalytic efficiency could be enhanced [30]. Studies of optical property of single-walled carbon nanotube (SWCNT)/ZnS hybrid structure have been made earlier by several researchers [31,32], but to our knowledge, so far no systematic study of photoluminescence (PL) spectrum with variable excitation wavelengths has been made.

Here, in this article we report a very simple chemical process to synthesise SWCNT/ZnS hybrid structure. The hybrid structure has been obtained adopting a simple chemical reaction method, carried out at room temperature and involves minimum time consumption, relative to the methods reported earlier [30,31]. We also report a PL study of SWCNT/ZnS hybrid structure for a wide range of excitation wavelengths, from 220 nm to 400 nm. The goal of the present work has been to prepare SWCNT/ZnS hybrid structure in a very lucid method and to study the visible luminescence characteristics of SWCNT for possible applications in biological imaging, sensors and fabrication of nanoelectronic devices. The characteristic PL emissions as reported in the present article can be explained by considering the charge flow from ZnS NCs onto the SWCNT walls.

2. Experimental

We have procured SWCNTs (1–2 nm outer diameter, length: 1–3 μm and purity >95%) from Chengdu Organic Chemicals Co. Ltd., Chinese Academy of Sciences and further purified them by heating in a Muffle furnace (Metrex Scientific Instruments (P) Ltd., India) at 350°C for 1 h and then soaking in 6 M HCl overnight, followed by sonication using Peizo-U-Sonic (250 W) ultrasonicator for 5 min, filtration over a 0.22 μm millipore membrane and washing thoroughly with de-ionised water until pH neutral. Pristine SWCNT samples are characterised by scanning electron microscopy (SEM), energy-dispersive X-ray (EDAX), X-ray diffraction (XRD), Raman spectroscopy, high resolution transmission electron microscopy (HRTEM) and UV-Vis spectroscopy. Through a simple wet chemical process, SWCNTs are enveloped with as-prepared ZnS nanoparticles. The chemicals used for the purification of SWCNTs as well as for the synthesis of hybrid structure are of Merck (GR grade) and have been utilised without further purification. To prepare SWCNT/ZnS hybrid, we have taken 20 mL of zinc nitrate solution and 10 mL of saturated solution of sodium sulphide in methanol. To the freshly prepared zinc nitrate solution, 9.4 mg of pure SWCNT has been added and stirred vigorously using a magnetic stirrer up to 1 h. Sodium sulphide solution is then added dropwise to the zinc nitrate solution containing SWCNTs till the pH become 8. Ultrasonication of the solution has been done for 1 h, followed by filtration using millipore filtration apparatus to separate the precipitate from the mixture. The precipitate is washed with methanol followed by de-ionised water to remove excess sodium particles. The above-mentioned process has been carried out at room temperature.

Characterisation of the as-prepared sample for its nanostructural as well as optical properties has been done by SEM/EDAX (HITACHI S-3000N) and XRD (Philips PANalytical X-Pert Pro diffractometer with CuKα radiation, $\lambda = 0.154056$ nm). Compositional analysis of the sample is done by Fourier transform infrared ray (FTIR) (Nicolet iS10) spectroscopy. FTIR analysis confirmed the presence of sulphur compound with SWCNTs. The microstructure of the surfaces of SWCNT bundles attached with ZnS nanoparticle has been confirmed by HRTEM (JEOL JEM 2100) micrograph using an operating voltage of 200 kV. Raman spectroscopy (provided with edge filter and a charge-coupled device (CCD) detector) has been performed using TRIAX 550 JY Horiba USA. Argon ion laser of wavelength 480 nm has been used as an excitation source for Raman spectroscopy. To study the optical property of SWCNT/ZnS hybrids, the dried sample is dispersed in dimethyl sulphoxide (DMSO) and its optical absorbance characteristics studied using UV-Vis (HITACHI U-3010) spectrophotometer. PL spectrum of the sample has been studied using FL spectrofluorimeter (HITACHI, F-2500).

3. Results and discussion

Figure 1(a) shows the SEM micrograph of SWCNT/ZnS hybrid. The inset of Figure 1(a) shows the HRTEM micrograph of pristine SWCNT. From Figure 1(a) it is observed that ZnS nanocrystallites have thick layers around aligned SWCNT bundles. The alignment, though achieved accidentally, may be assigned to the exfoliation of SWCNT bundles during sonication. The presence of ZnS has been revealed from EDAX analysis of modified SWCNT. EDAX spectrum of ZnS coated SWCNT is shown in Figure 1(b). The presence of zinc (Zn) and sulphur (S) along with carbon (C) indicates that ZnS is present with SWCNTs. The XRD pattern of the modified SWCNT/ZnS hybrid structure is shown in Figure 2. The peaks centred at 26°, 44° and 50° correspond to (0 0 2), (1 0 1) and (1 0 2) reflections, respectively, of graphitic planes of the CNTs (JCPDS card no. 75-1621). The XRD pattern of SWCNT/ZnS heterostructures also shows the peaks assigned to (1 1 1), (2 2 0) and (3 1 1) planes of the cubic phase of ZnS crystal structure which are in good agreement with the reported data for ZnS (JCPDS card no. 05-0566). The diffraction pattern reveals a mixture of the cubic (fcc) phase of ZnS with a lattice constant of $a = 5.4060$ Å and graphitic structure of SWCNTs. The broadening of the diffraction peaks reveals that ZnS nanocrystallites are formed. The average size of the crystallite is calculated from the full-width at half-maximum (FWHM) of the diffraction peaks using the following Debye–Scherrer formula [33].

$$D = 0.89\lambda/\beta\cos\theta,$$

where D is the mean grain size, λ is the X-ray wavelength, β is the FWHM of diffraction peak and θ is the diffraction angle. The average size of ZnS nanocrystallite is found to be 2 nm. The HRTEM picture clearly reveals the attachment of ZnS NCs on the surfaces of thinner SWCNT bundles. Figure 3 shows the HRTEM micrograph of SWCNT/ZnS hybrid structure. The inset of Figure 3 shows the corresponding selected area electron diffraction (SAED) image. The uniform concentric rings suggest that the NCs have preferential instead of random orientation. The concentric rings could be assigned as diffraction from (1 1 1), (2 2 0) and (3 1 1) planes of cubic ZnS from the centre most ring, respectively. The interplanar spacing (dhkl) as calculated from TEM, XRD and JCPDS

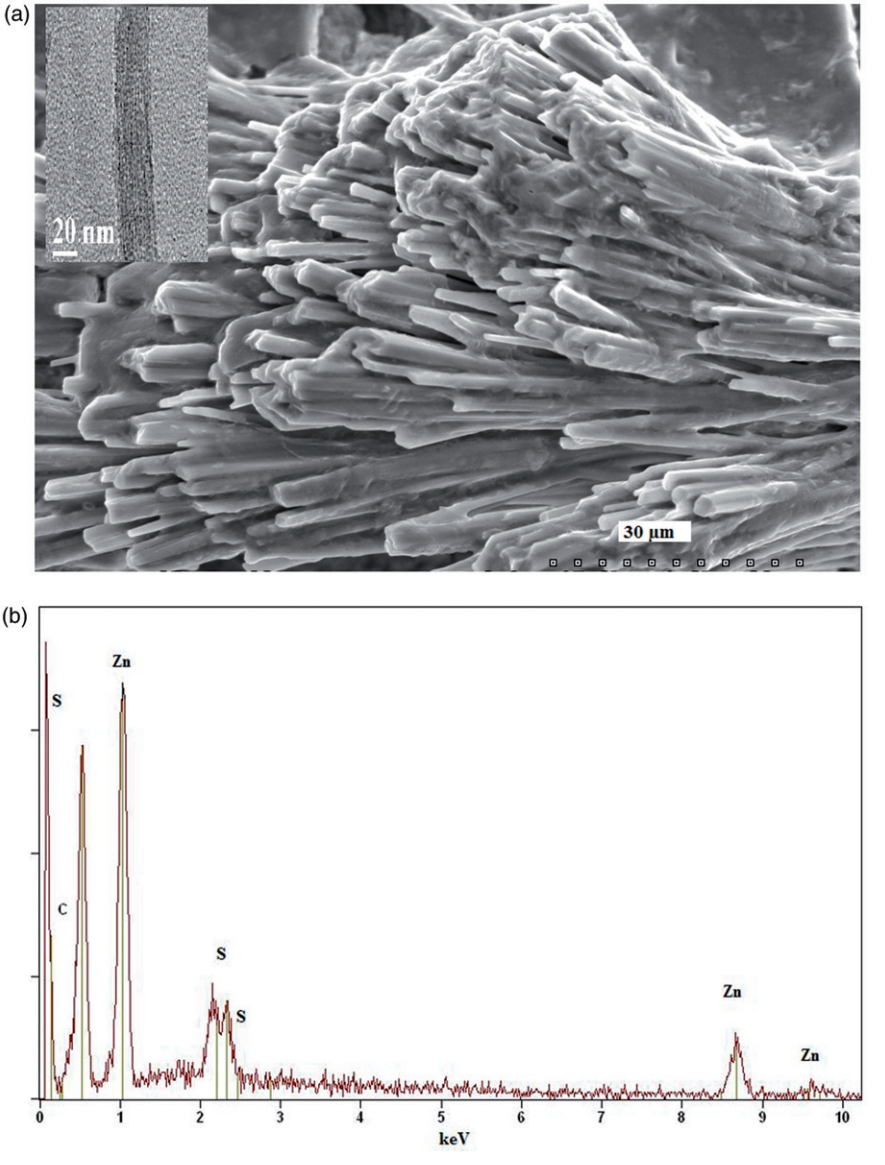

Figure 1. (a) SEM micrograph of SWCNT bundles in ZnS envelope; inset shows the HRTEM micrograph of pristine SWCNT bundle. (b). EDAX analysis of SWCNT/ZnS hybrid structure.

data card, and corresponding (hkl) values are summarised in Table 1. But the average size of the ZnS NCs from HRTEM micrograph is found to be 12 nm. Therefore, it may be concluded that the ZnS nanoparticles consist of smaller particles or subunits with the average size 2 nm. Clusters of nanoparticles formed may be due to the fact that no capping agent has been used in the method to control agglomeration.

The chemical state of SWCNT surface is characterised by FTIR spectroscopy. Figure 4 shows a comparison of the FTIR spectra of pristine SWCNT and that of SWCNT/ZnS

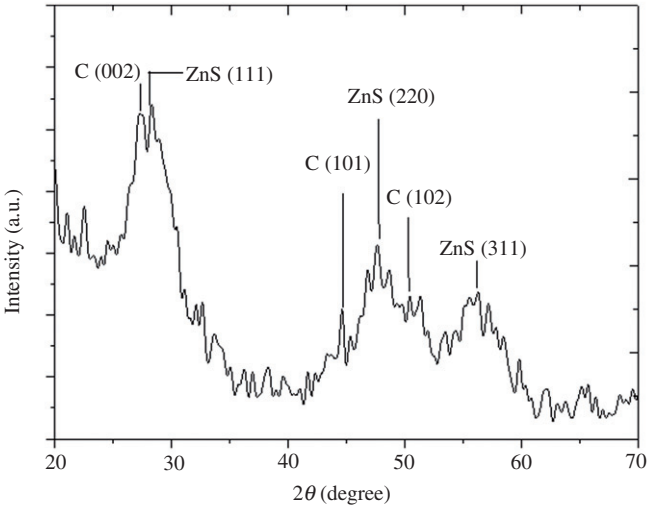

Figure 2. Smoothened XRD pattern of SWCNT/ZnS hybrid structure.

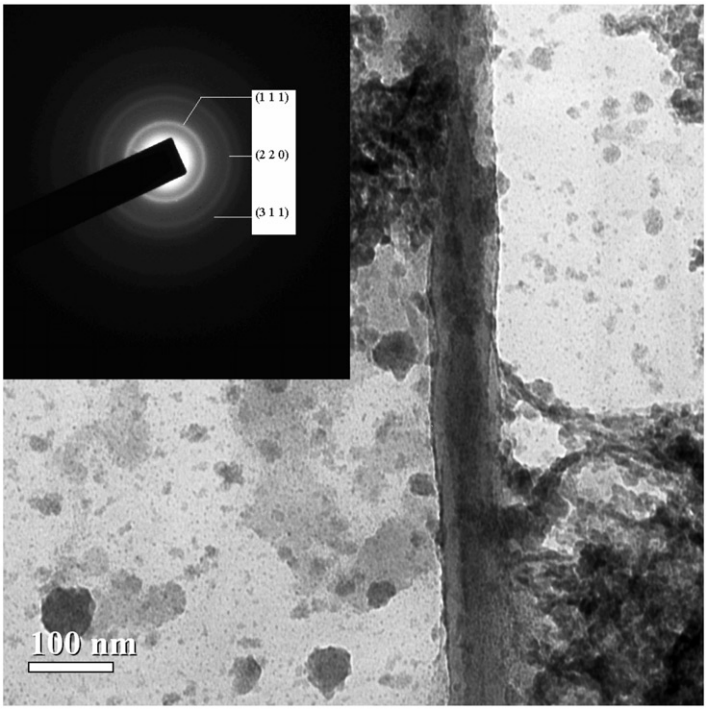

Figure 3. HRTEM micrograph showing SWCNT bundles hybridised with ZnS nanoparticles. The inset shows the SAED pattern of the modified SWCNT samples.

Table 1. Interplanar spacing (d_{hkl}) from TEM, XRD and JCPDS data with corresponding ($h\,k\,l$) values of ZnS NCs.

d_{TEM} (Å)	d_{XRD} (Å)	d_{JCPDS} (Å)	($h\,k\,l$)
3.129	3.150	3.123	(1 1 1)
1.871	1.912	1.912	(2 2 0)
1.600	1.637	1.633	(3 1 1)

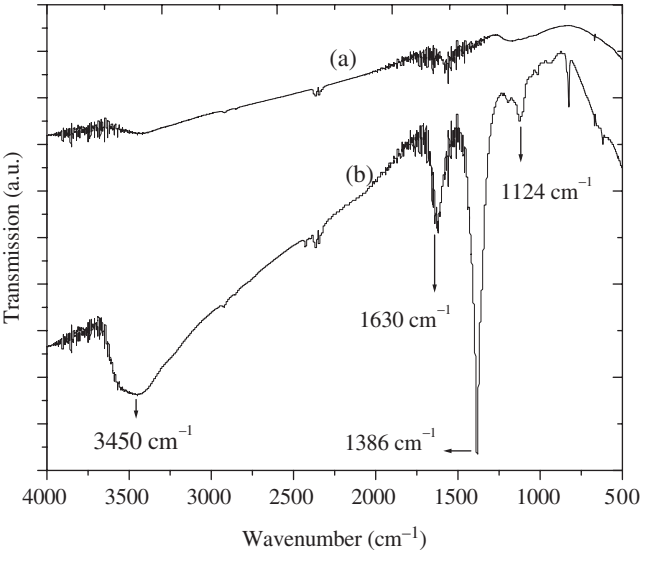

Figure 4. FTIR spectra of (a): pristine SWCNT, and (b) SWCNT/ZnS hybrid.

heterostructure. The stretches at 1124 and 1386 cm^{-1} confirm the presence of sulphur compound bondings, which are absent in the case of pristine SWCNT. Peaks at 1630 and 3540 cm^{-1} are deformation vibrations and stretching vibrations of H_2O, respectively, originated from the absorption of water by KBr matrix [34]. In order to investigate the effect of semiconductor NC adhesion to the SWCNT bundles, Raman spectra of pristine SWCNT and SWCNT/ZnS hybrid structure are recorded. Figure 5 shows the comparison of Raman spectra for both samples. In the Raman spectra, D and G modes for both pristine and hybridised SWCNTs are located at 1359 cm^{-1} and 1589 cm^{-1}, respectively. Also, no appreciable shift of SWCNT/ZnS hybrid structure in the radial breathing mode (RBM) has been observed when compared to that of the pristine SWCNT samples. So, hybrid structure remained almost unaffected, as reported earlier [31]. The spikes present along with the Raman peaks do not correspond to Raman emission. The CCD array detectors are susceptible to the effects of cosmic rays that pass through them during an exposure. These rays add charge to one or more pixels depending on the direction of travel of the ray and hence the spikes which appeared in the observed Raman spectra.

The absorbance spectrum of pristine as well as ZnS–SWCNT hybrid structure is shown in Figure 6. Characteristic UV-Vis absorption has been observed with a strong absorbance

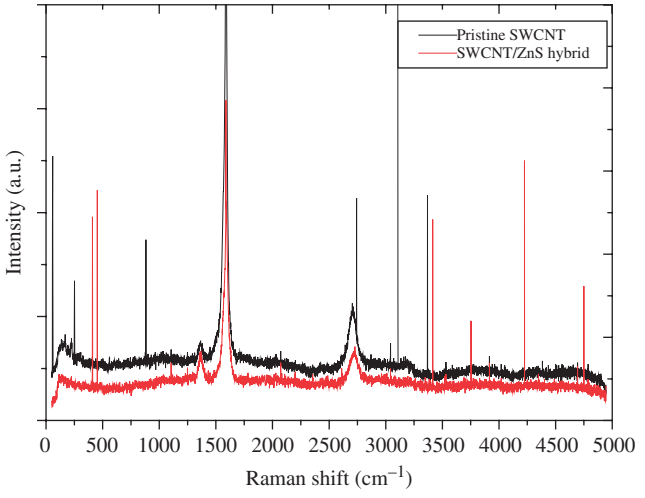

Figure 5. Raman spectra of pristine SWCNT and SWCNT/ZnS hybrid.

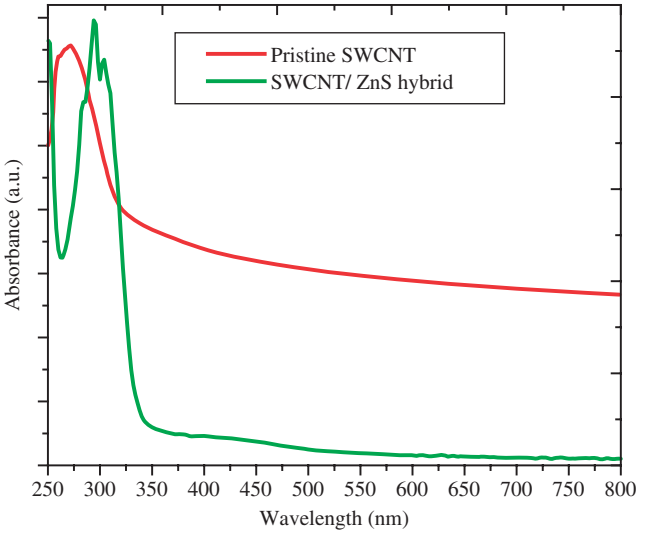

Figure 6. Absorbance spectra of pristine SWCNT and SWCNT/ZnS hybrid.

peak at about 296 nm for SWCNT/ZnS hybrid while at about 271 nm for pristine SWCNT samples. The absorbance peak of SWCNT/ZnS hybrid is red shifted relative to that of the pristine SWCNT because the coating of ZnS NCs on SWCNT walls has increased the total size of the bundles. When compared to the absorbance of bulk zinc blende ZnS (340 nm), a blue shift is noticed, which is due to quantum size effects [32]. We have not observed any absorption bands in the Vis-NIR region for pristine SWCNTs as reported earlier by Strano et al. [22], may be due to the fact that exfoliation of SWCNT bundles in DMSO has not taken place up to that extent as acquired by dispersing them

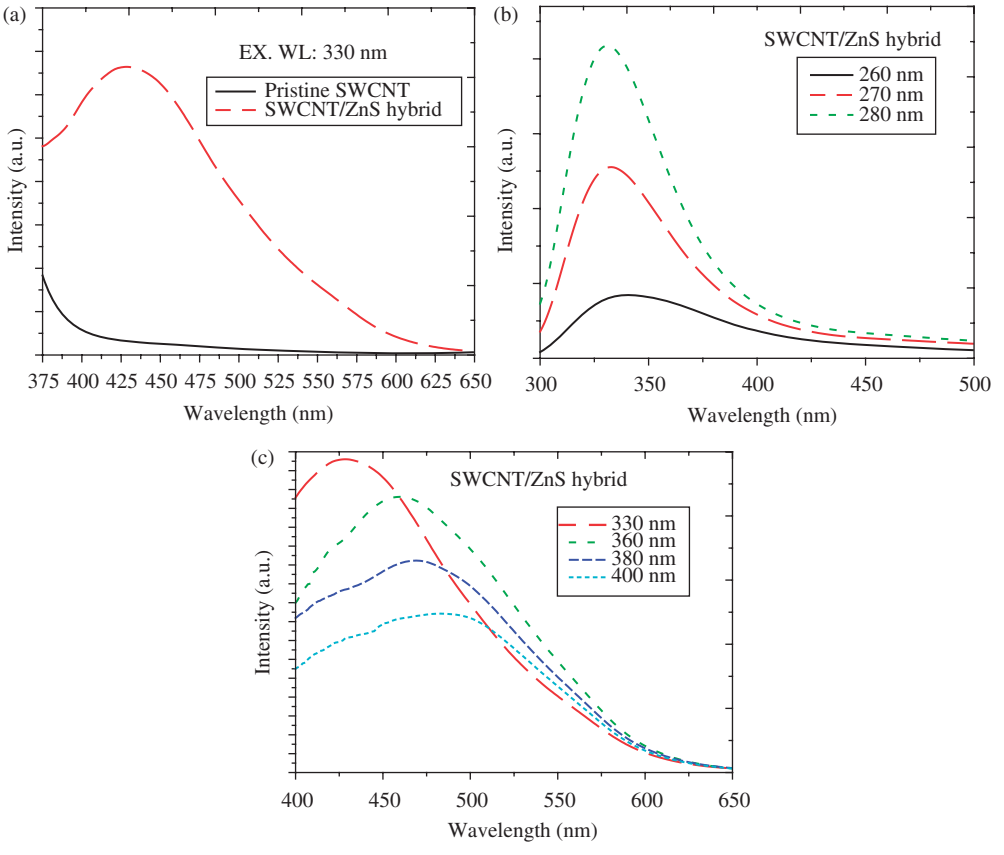

Figure 7. (a) PL spectra of pristine SWCNT and SWCNT/ZnS hybrid (at excitation of 330 nm wavelength). (b) First range of PL emission (at excitation of 260–280 nm wavelength). (c) Second range of PL emission (at excitation of 330–400 nm wavelength).

in sodium dodecyl sulphate (SDS). Figure 7(a) shows the PL spectra of pristine SWCNT and SWCNT/ZnS hybrid structure at an excitation wavelength of 330 nm. The SWCNT/ZnS hybrid showed a broad emission in the visible region covering up to 650 nm with peak emission at 425 nm under excitation of 330 nm, which is absent in the case of pristine SWCNT sample. Figure 7(b) and (c) exhibits the two typical patterns of PL spectra for two different ranges of excitation wavelengths, one for 260–280 nm and another for 330–400 nm excitation wavelength ranges. Below 260 nm excitation wavelength, no pronounced emission is being observed. When the hybrid sample is excited by low excitation wavelengths from 260 to 280 nm, PL bands gradually blue shifted. For 260 nm excitation wavelength, the emission peak is found at 336 nm, for 270 nm, the peak happened to be at 333 nm and for 280 nm excitation wavelength, the peak has been found to be at 330 nm.

The emission pattern begins to change its nature with the 330 nm excitation wavelength. For 330 nm excitation, we get the emission peak at 430 nm. For 360 nm excitation wavelength, we get a peak at 460 nm, for 380 nm excitation, the peak has been observed to be at 470 nm and finally for 400 nm excitation wavelength, the peak positioned

at 495 nm. In this case, unlike for low excitation wavelengths, the PL peak positions are gradually red shifted and decreased in intensity with increasing excitation wavelengths. On further increasing the excitation wavelength, no appreciable emission has been obtained.

Due to the direct adhesion of ZnS NCs with SWCNTs, some local energy levels in the bandgap are formed [32]. When irradiated by UV light, valence band electrons of ZnS get excited and move towards the conduction band forming electron–hole pairs. Due to strong interfacial connection between ZnS nanoparticles and SWCNTs, the excited e^- of the conduction band of ZnS nanoparticles migrate to SWCNTs, which are relatively good electron acceptors [35–37]. So, recombination of the electron–hole pairs get retarded, which results in the promotion of photocatalytic activity in ZnS nanoparticles [30], as well as modification of energy band structure. When excited by lower excitation wavelengths and hence higher energy values, transition of electrons from ZnS to SWCNTs takes place, but these high energetic electrons transit instantly thereby causing emission. Up to 280 nm excitation wavelength, the number of electrons taking part in the transition process increases and hence the increase in PL intensity. But on further exciting the hybrid structure with increased wavelengths, electrons get trapped by SWCNTs and intra-band emission takes place. Retardation of electron–hole pair formation increases, leading to decrease in intensities and gradual red shift.

4. Conclusions

Synthesis of SWCNT/ZnS heterostructures consisting of ZnS NCs of average size 2 nm has been achieved following a very simple chemical precipitation method without using any capping agent. The NCs wrapped around the thin SWCNT bundles is confirmed by HRTEM, SEM and XRD studies for SWCNT/ZnS hybrid structure. The FTIR analysis implies that the ZnS nanoparticles are deposited on the surface groups of SWCNTs. At UV excitation of 330 nm, significant visible PL has been observed with ZnS–SWCNT hybrid structure. Furthermore, two distinct patterns of PL spectrum have also been observed when excited by UV radiations of increasing wavelengths. Therefore the present method is a lucid method to synthesise SWCNT/metal-sulphide hybrid structure and can also be implemented to obtain varieties of CNT/metal-sulphide heterostructures.

Acknowledgements

The authors gratefully acknowledge the support from Dr D. Sukul and Dr A.K. Patra of Department of Chemistry, NIT Durgapur, for PL and FTIR characterisation. They are grateful to Technical Education Quality Improvement programme (TEQIP), NIT Durgapur and Government of India for the financial support and maintenance of Institute Research Fellowship. They extend their thanks to CRF, IIT Kharagpur, for making available the HRTEM facility. They also extend their sincere thanks to Dr A. Roy, IIT Kharagpur for Raman spectroscopy.

References

[1] S. Iijima, *Helical microtubules of graphitic carbon*, Nature 354 (1991), pp. 56–58.
[2] M.S. Dresselhaus, G. Dresselhaus, and P. Avouris (eds.), *Carbon Nanotubes: Synthesis, Structure, Properties and Applications*, Vol. 80, Springer, Berlin, 2001.

[3] (a) S. Banerjee, M.J.C. Khan, and S.S. Wong, *Rational chemical strategies for carbon nanotube functionalization*, Chem. Eur. J. 9 (2003), pp. 1898–1908; (b) K.S. Coleman, A.K. Chakraborty, S.R. Bailey, J. Sloan, and M. Alexander, *Iodination of single-walled carbon nanotubes*, Chem. Mater. 19 (2007), pp. 1076–1081; (c) J. Chen, S. Chen, X. Zhao, L.V. Kuznetsova, S.S. Wong, and I. Ojima, *Functionalized single-walled carbon nanotubes as rationally designed vehicles for umor-targeted drug delivery*, J. Amer. Chem. Soc. 130(49) (2008), pp. 16778–16785; (d) A.K. Chakraborty, K.S. Coleman, and V.R. Dhanak, *The electronic fine structure of 4-nitrophenyl functionalized single-walled carbon nanotubes*, Nanotechnology 20 (2009), pp. 155704–155709.

[4] M.J. O'Connell, S.M. Bachilo, C.B. Huffman, V.C. Moore, M.S. Strano, E.H. Haroz, K.L. Rialon, P.J. Boul, W.H. Noon, C. Kittrell, J. Ma, R.H. Hauge, R.B. Weisman, and R.E. Smalley, *Bandgap fluorescence from individual singlewalled carbon nanotubes*, Science 297(5581) (2002), pp. 593–596.

[5] S. Lebedkin, K. Arnold, F. Hennrich, R. Krupke, B. Renker, and M.M Kappes, *FTIR–luminescence mapping of dispersed single-walled carbon nanotubes*, New J. Phys. 5 (2003), pp. 140.1–140.11.

[6] M. Olek, T. Busgen, M. Hilgendorft, and M. Ciersig, *Quantum dot modified multiwall carbon nanotubes*, J. Phys. Chem. B 110 (2006), pp. 12901–12904.

[7] A. Profumo, M. Fagnoni, D. Merli, E. Quartarone, S. Protti, and D. Dondi, *Multiwalled carbon nanotubes chemically modified gold electrode for inorganic as speciation and Bi(III) determination*, Anal. Chem. 78 (2006), pp. 4194–4199.

[8] Y.B. Zhao, T.T. Chen, J.H. Zou, and W.F. Shi, *Fabrication and characterization of monodisperse zinc sulfide hollow spheres by gamma-ray irradiation using PSMA spheres as templates*, J. Cryst. Growth 275 (2005), pp. 521–527.

[9] S. Banerjee and S.S. Wong, *In situ growth of 'fused', ozonized single-walled carbon nanotube—quantum dot junctions*, Adv. Mater. 16 (2004), pp. 34–37.

[10] Y. Yang, H.Y. Wang, X.F. Lu, Y.Y. Zhao, X. Li, and X. Wang, *Electrospinning of carbon/CdS coaxial nanofibers with photoluminescence and conductive properties*, Mater. Sci. Eng. B 40 (2007), pp. 48–52.

[11] H. Kim and W. Sigmund, *Zinc sulfide nanocrystals on carbon nanotubes*, J. Cryst. Growth 255 (2003), pp. 114–118.

[12] N. Cho, K.C. Choudhury, R.B. Thapa, Y. Sahoo, T. Ohulchansky, and A.N. Cartwright, *Efficient photodetection at IR wavelengths by incorporation of PbSe-carbon-nanotube conjugates in a polymeric nanocomposite*, Adv. Mater. 19 (2007), pp. 232–236.

[13] Y. Liu and L. Gao, *In situ coating multiwalled carbon nanotubes with CdS nanoparticles*, Mater. Chem. Phys. 91 (2005), pp. 365–369.

[14] I. Robel, B.A. Bunker, and P.V. Kamet, *SWCNT-CdS nanocomposite as light harvesting assembly: Photoinduced charge transfer interactions*, Adv. Mater. 17 (2005), pp. 2458–2463.

[15] M.C. Daniel and D. Astruc, *Gold Nanoparticles: Assembly, supramolecular chemistry, quantum-size related properties, and applications towards biology, catalysis and nanotechnology*, Chem. Rev. 104(1) (2004), pp. 293–346.

[16] J. Kong, N.R. Franklin, C.W. Zhou, M.G. Chapline, S. Peng, K.J. Cho, and H.J. Dai, *Nanotube molecular wires as chemical sensors*, Science 287(5453) (2000), pp. 622–625.

[17] M.A. Correa-Duarte, J. Perez-Juste, A. Sanchez-Iglesias, M. Giersig, and L.M. Liz-Marzan, *Aligned assemblies of Au nanorods using carbon nanotubes as templates*, Angew. Chem. Int. Ed. 44(28) (2005), pp. 4375–4378.

[18] M.A. Correa-Duarte, M. Grzelezak, V. Salgureirino-Maceira, M. Giersig, L.M. Liz-Marzan, M. Farle, K. Sierazdki, and R.J. Diaz, *Alignment of carbon nanotubes under low magnetic fields through attachment of magnetic nanoparticles*, J. Phys. Chem. B 109(41) (2005), pp. 19060–19063.

[19] N. Tessler, V. Medvedev, M. Kazes, S.H. Kan, and U. Banin, *Efficient near-infrared polymer nanocrystal light-emitting diodes*, Science 295(5559) (2002), pp. 1506–1508.
[20] J.H. Planeix, N. Coustel, B. Coer, V. Brotons, P.S. Kumbhar, R. Dutartre, P. Genesre, and P.M. Ajayan, *Application of carbon nanotubes as supports in heterogeneous catalysis*, J. Amer. Chem. Soc. 116(17) (1994), pp. 7935–7936.
[21] J. Cao, J.Z. Sun, H. Heng, H.Y. Li, H.Z. Chen, and M. Wang, *Carbon Nanotube/CdS Core-Shell nanowires Prepared by a simple room-temperature chemical reduction method*, Adv. Mater. 16(1) (2004), pp. 84–87.
[22] M.S. Strano, C.A. Dyke, M.L. Usrey, P.W. Barone, M.J. Allen, H.W. Shan, C. Kittrell, R.H. Hauge, J.M. Tour, and R.E. Smalley, *Electronic structure control of single-walled carbon nanotube functionalization*, Science 301(5639) (2003), pp. 1519–1522.
[23] W. Tang and D.C. Cameron, *Electroluminescent zinc sulphide devices produced by sol-gel processing*, Thin Solid Films 280(1–2) (1996), pp. 221–226.
[24] T.V. Prevenslik, *Acoustoluminescence and sonoluminescence*, J. Lumin. 87 (2000), pp. 1210–1212.
[25] P. Calandra, M. Goffredi, and T.V. Liveri, *Study of the growth of ZnS nanoparticles in water/AOT/n-heptane microemulsions by UV-absorption spectroscopy*, Colloid Surf. A – Physicochem. Eng. Asp. 160(1) (1999), pp. 9–13.
[26] X.L. Wang, S.O. Pehkonen, and A.K. Ray, *Removal of Aqueous Cr (VI) by a Combination of Photocatalytic Reduction and Coprecipitation*, Ind. Eng. Chem. Res. 43(7) (2004), pp. 1665–1672.
[27] D. Jie, J. Zhengjing, L. Wenge, B. Guoqing, and Z. Qinyu, *Solvothermal preparation of inorganic–organic hybrid compound of* $[(ZnS)_2(en)]_\infty$ *and its application in photocatalytic degradation*, Mater. Lett. 55(6) (2002), pp. 383–387.
[28] S. Yanagida, K. Mizumoto, and C. Pac, *Semiconductor photocatalysis. Part 6. Cis-trans photoisomerization of simple alkenes induced by trapped holes at surface states*, J. Amer. Chem. Soc. 108(4) (1986), pp. 647–654.
[29] Y. Changhui, F. Xiaosheng, L. Guanghai, and Z. Lide, *Origin of the green photoluminescence from zinc sulfide nanobelts*, Appl. Phys. Lett. 85(11) (2004), pp. 3035–3037.
[30] F. Shou-ai, Z. Jian-hong, and Z. Zhen-ping, *The manufacture of carbon nanotubes decorated with ZnS to enhance the ZnS photocatalytic activity*, New Carbon Mater. 23 (2008), pp. 228–234.
[31] M. Nath, P.V. Teradesai, D.V.S. Muthu, A.K. Sood, and C.N.R. Rao, *Single-walled carbon nanotube bundles intercalated with semiconductor nanoparticles*, Curr. Sci. 85 (2003), pp. 956–960.
[32] F. Gu, C. Li, and S. Wang, *Solution-chemical synthesis of carbon nanotube/ZnS nanoparticle core/shell heterostructures*, Inorg. Chem., 46(13) (2007), pp. 5343–5348.
[33] B.D. Cullity, *Elements of X-ray Diffraction*, 2nd ed., Addison-Wesley Company, Reading, USA, p. 102.
[34] Y. Zhao, H. Liu, F. Wang, J. Liu, K. Park, and M. Endo, *A simple route to synthesize carbon nanotube/cadmium-sulfide hybrid heterostructures and their optical properties*, J. Solid State Chem. 182 (2009), pp. 875–880.
[35] Y. Sun, S.R. Wilson, and D.I. Schuster, *High dissolution and strong light emission of carbon nanotubes in aromatic amine solvents*, J. Amer. Chem. Soc. 123 (2001), pp. 5348–5349.
[36] P. Serp, M. Corrias, and P. Kalack, *Carbon nanotubes and nanofibers in catalysis*, Appl. Catal. A – Gen. 253 (2003), pp. 337–358.
[37] W. Fei, Z. Qiang, and Q. Wei-Zhong, *Progress on aligned carbon nanotube arrays*, New Carbon Mater. 22 (2007), pp. 271–282.